IEEE Access
Multidisciplinary | Rapid Review | Open Access Journal

Received 13 October 2023, accepted 4 November 2023, date of publication 8 November 2023,
date of current version 13 November 2023.

Digital Object Identifier 10.1109/ACCESS.2023.3331016

RESEARCH ARTICLE

Unbalanced Distribution System Expansion and Energy Storage Planning Under Wildfire Risk

AUGUSTO ZANIN BERTOLETTI, (Member, IEEE), AND JOSUE CAMPOS DO PRADO, (Member, IEEE)
School of Engineering and Computer Science, Washington State University Vancouver, Vancouver, WA 98686, USA
Corresponding author: Josue Campos do Prado (josue.camposdoprado@wsu.edu)

ABSTRACT Reducing the risks of wildfire ignition has become a major concern for many electric utilities. In recent years, they have relied on Public Safety Power Shutoff (PSPS) programs to de-energize select power lines to prevent wildfire risks. A cost-effective solution for the power distribution system expansion planning in regions with increased wildfire risk could be achieved by jointly combining new distribution lines and energy storage systems (ESSs) while taking into account the overhead distribution lines availability given the increasing number of PSPS events. This paper proposes a two-stage stochastic optimization approach for the expansion planning of a power distribution system under wildfire risk with a compliance check on unbalanced power flow and system operation limits. The resulting model is a mixed-integer linear programming (MILP) optimization problem. The proposed model is validated on a modified version of the IEEE 13-node system and the IEEE 123-node system. Simulation experiments and sensitivity analysis are performed to validate the effectiveness of the proposed formulation using different High Fire-Threat District (HFTD) Tier Zones based on real-world data from electric utilities in California.

INDEX TERMS Energy storage systems (ESSs), power system planning, unbalanced distribution systems, wildfires.

NOMENCLATURE

INDICES AND SETS

Ω_i	Set of lines connected to node i.
$\phi \in \Phi_i$	Phases of node i.
$\xi \in \Xi$	Set of scenarios.
L	Set of distribution lines.
L^E	Set of existing distribution lines.
$s \in S$	Representative periods of the year.
$i, j, k \in I$	Index of nodes.

VARIABLES

$\mathbf{P_i^{shed,\phi}}$	Active power shed at node i and phase ϕ.
$\mathbf{P_G}$	Three-phase active power from the substation.
$\mathbf{S_{i,j} = P_{i,j} + jQ_{i,j}}$	Three-phase complex power flow from node i to j.
$\mathbf{W_i}$	Three-phase voltage magnitude square vector at node i.
$p_{G_i}^{\phi\ \phi}$	Real power dispatch of DGs at node i, for phase $\phi \in \Phi_i$.
$P_{L_i}^{\phi} + jQ_{L_i}^{\phi}$	Complex power demand at node i, for phase $\phi \in \Phi_i$.
$u_{i,j}$	Line availability.
$w_{i,j}$	Binary variable, $w_{i,j} = 1$ if the line is built, $w_{i,j} = 0$ otherwise.
β_i	Number of ESS at node i.
$E_{b_i}^{\phi}$	Energy stored in ESS at node i and phase ϕ.
$P_{b_i}^{\phi}$	Active power of ESS at node i and phase ϕ.
$P_{c_i}^{\phi}$	Active charging power of ESS at node i and phase ϕ.
$P_{d_i}^{\phi}$	Active discharging power of ESS at node i and phase ϕ.
$Q_{b_i}^{\phi}$	Reactive power of ESS at node i and phase ϕ.

The associate editor coordinating the review of this manuscript and approving it for publication was Salvatore Favuzza.

CONSTANTS

Δt	Time step.
κ_i	Energy price at node i.
κ_{ESS}	Investment cost of an ESS module.
$\mathbf{Z_{i,j}}$	Phase-impedance matrix of a line, from node i to j.
π_ξ	Probability of realizing scenario ξ.
σ_s	Weight of the time window s.
E_0	Initial energy stored in ESS.
$K_{i,j}$	Investment cost of building line from node i to j.
M	Large enough positive constant.
N	Number of years.
OM_{ESS}	Operation and maintenance cost for an ESS module.
$S_{b_i}^{max,\phi}$	Maximum apparent power capacity of ESS at node i and phase ϕ.
$S_{i,j}^{max}$	Maximum apparent power capacity of the line from node i to j.
T_s	Number of hours of the representative time window s.
$v_{lb} = 0.9$	Voltage lower bound limit (in p.u.).
$v_{ub} = 1.1$	Voltage upper bound limit (in p.u.).
$VoLL$	Value of lost load ($/kWh).

I. INTRODUCTION

A. BACKGROUND AND MOTIVATION

The recent increase in wildfire activity poses a danger to the safe and reliable operation of electrical power systems around the world. The year of 2020, in particular, was marked by several extremely severe wildfires, setting records in the Arctic [1], Australia [2], Brazil [3] and western United States (U.S.) [4].

Wildfires can be naturally caused or human-induced, and there are many studies suggesting that climate change has been a key factor in increasing the risk and extent of wildfires in several regions [5], [6], [7], [8], [9], [10], [11]. In the year of 2021 alone, the National Center for Environmental Information (NCEI) reported an estimate cost of $10.4 billion due to wildfires across the United States [12].

Wildfires are expected to become more frequent and severe in many regions [13], [14]. Therefore, energy providers must be proactive and forward-thinking to ensure that their operations, workforce, and long-term strategic plans are prepared for and equipped to handle this growing external threat [15]. In order to prevent wildfires caused by electrical equipment, utilities in Western United States have relied on Public Safety Power Shutoff (PSPS) events to de-energize select transmission and distribution lines to avoid wildfires during certain weather conditions. De-energization decisions take into account several input parameters, including meteorological conditions (e.g., humidity, temperature, and wind speed and direction), fuel conditions (e.g., dry material on the ground and vegetation near power lines) [16], and wildfire risk metrics (e.g., Fosberg Fire Weather Index and Keetch-Byram Drought Index) [17].

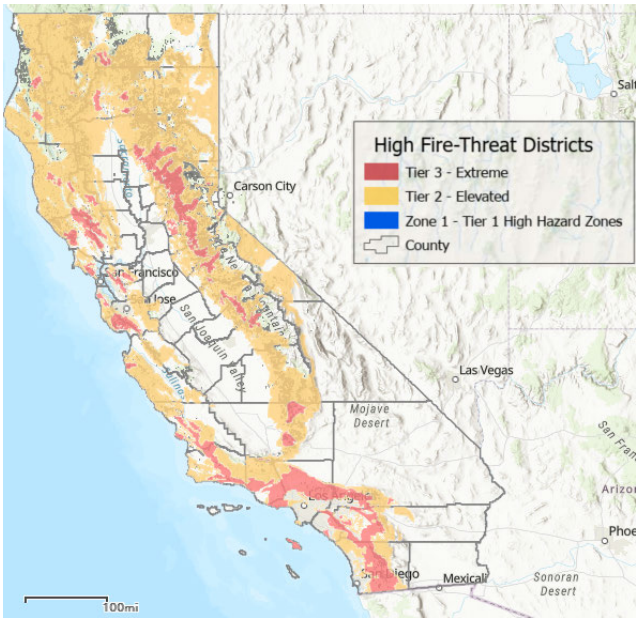

FIGURE 1. CPUC High Fire-Threat District Map [18].

In 2012, the California Public Utilities Commission (CPUC) created a statewide map designed to show areas where there is an increased risk for utility-associated wildfires in the state of California [18]. The map is divided into 3 Tiers: Tier 1 High Hazard Zones are zones near communities, roads, and utility lines, and are a direct threat to public safety, Tier 2 fire-threat areas outline areas where there is a higher risk from utility related wildfires, and Tier 3 fire-threat areas outline areas where there is an extreme risk from utility-related wildfires. The map developed by CPUC is presented in Fig. 1. By using PSPS historical data within different HFTD zones, one can estimate the expected frequency and duration of power line outages without the need of modeling and correlating weather parameters, fuel conditions, and wildfire risks metrics, which are generally complex tasks.

To date, utility reports indicate the number and location of customers affected by equipment de-energization. Customers may be located in Tier 2 or Tier HFTD zones, or outside of any zone. Since PSPSs events are mainly concentrated in Tier 2 and Tier 3 zones, residing in or near these zones increases the likelihood of experiencing PSPS-related outages [19]. Vegetation contact is reported as the highest contributor for the risk for HFTD distribution, but equipment/facility failure is the highest contributor for transmission and non-HFTD distribution, where over 90% of wildfire risk comes from HFTD distribution [20].

Understanding that de-energizing customers causes not only significant disruption but also safety risks to those impacted, and considering both risk reduction from wildfires and PSPSs, Pacific Gas & Electric (PG&E) stipulated a

goal to significantly increase underground miles annually, ramping up to 1,200 miles or more of undergrounding per year by 2026 [20]. Although utilities are working on different alternatives to reduce the impact of PSPSs through microgrids, segmentation, and resiliency zones in the short term, the long-term climate models point to a higher probability of more frequent fire weather conditions. Therefore, it is expected that the absolute number of PSPS events will not change, and may even increase in future years [20].

B. LITERATURE REVIEW

Several power distribution grid expansion planning models have been proposed in the literature. References [21], [22], and [23] provided comprehensive reviews and surveys of existing works. However, the majority of such works assumed normal power grid conditions and neglected the potential impacts of high impact low-probability (HILP) events, such as wildfires, on grid expansion decisions.

More recently, some works have incorporated the risks and impacts of wildfires in power system operation and planning problems. On the operation side, most of the existing works focused on distribution network operation during a progressive wildfire. The first work in this regard modeled the heat transfer from an approaching wildfire and its impact on the dynamic line rating (DLR) of a power distribution line [24]. The work in [25] expanded the previous heat transfer model to consider the non-steady state heat balance equation on the DLR modeling. Some recent works [26], [27], [28] used the same wildfire progression model to investigate select operation strategies, including network reconfiguration and the deployment of distributed generation and energy storage systems, to improve the distribution system resilience during such events. In [29], the authors integrated the DLR of transmission lines into the optimal power flow model to reduce the risk of wildfire ignitions. An attacker-defender approach for the optimal operation of a transmission network subjected to the risks of a progressing wildfire was proposed in [30].

On the planning side, most of the existing literature focused on the development of short-term mathematical models for optimal scheduling of PSPSs during wildfire season [31], [32]. The work in [33] presented a framework to select transmission lines to de-energize in order to balance wildfire risk reduction, total load shedding, and fairness considerations. The authors in [34] proposed a multi-period optimization formulation to locate and size infrastructure investments for the transmission system expansion problem. The PSPSs were simultaneously chosen to minimize wildfire ignition risk and load shedding, utilizing a weighting factor between both objectives. Stochastic and robust transmission expansion planning approaches considering wildfire risk were proposed in [35] and [36], respectively.

However, the aforementioned works have neither investigated the optimal expansion planning of unbalanced distribution systems under wildfire risk nor considered the optimal planning of energy storage systems (ESSs) to mitigate the impacts of PSPS events.

C. CONTRIBUTIONS

In contrast to existing works, this paper proposes a distribution system expansion planning framework considering the presence of HFTD Zones and the expected frequency and duration of PSPS-related outages to jointly determine new lines to be built and the optimal sitting and sizing of ESSs. The proposed framework is modeled as a two-stage stochastic optimization problem considering planning decisions in the first stage and the distribution system operation in the second stage. The model includes an objective function to minimize the planning costs subject to a set of constraints which include the linearized unbalanced power flow constraints and system operation limits, with a linear formulation for the optimal battery charging-discharging dynamics that respects the state-of-charge (SoC) limits without using complementary constraints. Moreover, random moments within the wildfire season are generated to characterize PSPS events, for the average number of hours given the HFTD Tier Zone.

Table 1 compares the proposed work with the existing literature on power system planning and operation under wildfire risk. The unique contributions of this paper are summarized as follows:

1) It presents an unbalanced distribution system expansion planning approach under wildfire risk. The proposed approach accounts for the possibility of lines and nodes being unavailable in high fire-threat districts (HFTD) during the wildfire season. Using historical data, the method aims to balance load shedding and expansion planning decisions, considering new overhead and underground distribution lines, through a stochastic optimization framework.
2) The optimal siting and sizing of ESSs are considered in the planning decisions to mitigate the impact of PSPSs events in distribution networks.

The rest of this paper is organized as follows. Section II describes the mathematical formulation of the proposed model. Section III presents relevant case studies. Finally, Section IV presents the main conclusions and recommendations for future work.

II. MODEL DESCRIPTION

A. ASSUMPTIONS AND DECISION-MAKING FRAMEWORK

The proposed methodology for the optimal distribution system expansion planning under wildfire risk is summarized in Fig. 2.

Initially, historical PSPS data is collected, and potential lines and ESS candidate nodes are chosen. Given that PSPS is a preventive measure based on several criteria, such as wind speed, humidity, Fire Potential Index (FPI), and others, the historical PSPS data reflects the occurrence of high-fire wildfire risk conditions, thus the average outage time within

TABLE 1. Comparison of the proposed work with the existing literature.

Scope	Type of problem	Planning/Operation Decisions	Reference
Transmission	PSPS Planning	De-energization scheduling	[31]–[33]
		De-energization scheduling and infrastructure enhancement	[34]
	Expansion Planning	New transmission lines	[35]
		New transmission lines, hardening, and distributed generation sitting	[36]
	Operation	Transmission network dispatch under wildfire risk	[29], [30]
Distribution		Distribution network dispatch under a progressing wildfire	[24]–[28]
	Expansion Planning	New distribution lines and ESS sitting and sizing	This Work

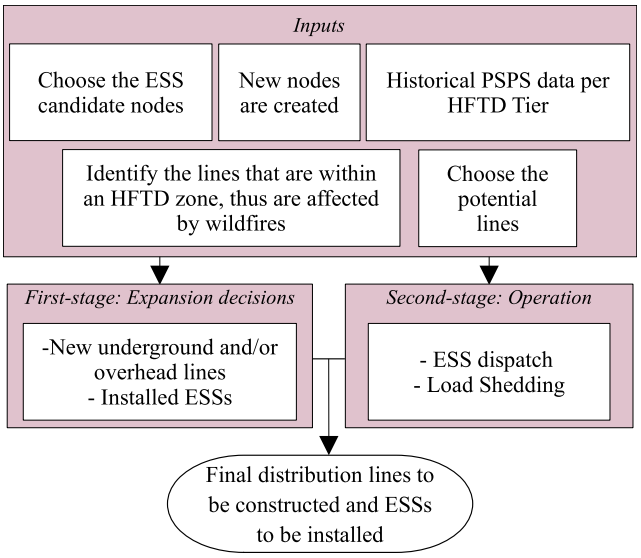

FIGURE 2. Flowchart of the proposed methodology.

HFTD tier zones and the number of events per year, are used to generate the scenarios to be used in the stochastic programming model.

The first-stage decisions comprise the sum of investment on new potential distribution lines and the cost of installing ESSs at the selected candidate nodes. Underground lines are assumed not to be affected by wildfires. In the second stage, the model minimizes the cost of operating and maintaining ESSs, the cost of energy, and the cost of shedding load at each node considering that the overhead lines within HFTD tier zones are not available due to wildfire risk.

B. MATHEMATICAL FORMULATION

The proposed two-stage stochastic optimization model is presented as follows:

$$\begin{aligned}\underset{\chi_{\{i,j\}},P_G,P_{shed}}{\text{Minimize}} \quad & \sum_{\forall w_{i,j}\in L^N} w_{i,j} * K_{i,j} + \kappa_{ESS} * \sum_{i=1}^{I} \beta_i \\ & + 365 * N * \sum_{i=1}^{I} \beta_i * OM_{ESS} \\ & + N * \sum_{\forall \xi \in \Xi} \pi_\xi \sum_{\forall s\in S,t} \sigma_S \sum_{\forall t=1}^{T_s} (P^G_{\xi,s,t} * \kappa_{\xi,s,t} + P^{shed}_{\xi,s,t} * VoLL)\end{aligned} \tag{1}$$

where,

$$P^{shed}_{\xi,s,t} = \sum_{\forall i\in I,\phi\in\Phi} P^{shed,\phi}_{i_{\xi,s,t}} \tag{2}$$

subject to:

$$\begin{aligned}P^{\phi}_{ij,\xi,s,t} = & \sum_{k:j\to k,\forall j\in\Omega_j} P^{\phi}_{jk,\xi,s,t} + P^{\phi}_{L_j,\xi,s,t} \\ & + P^{\phi}_{b_j,\xi,s,t} + p^{\phi}_{G_{j,s,t}} \\ & \forall\phi\in\Phi_i, \forall ij, jk, \xi, s, t\end{aligned} \tag{3}$$

$$\begin{aligned}Q^{\phi}_{ij,\xi,s,t} = & \sum_{k:j\to k,\forall j\in\Omega_j} Q^{\phi}_{jk,\xi,s,t} + Q^{\phi}_{L_j,\xi,s,t} \\ & + Q^{\phi}_{b_j,\xi,s,t}\ \forall\phi\in\Phi_i, \forall ij, jk, \xi, s, t\end{aligned} \tag{4}$$

$$\begin{aligned}\boldsymbol{W_{i,\xi,s,t}} - \boldsymbol{W_{j,\xi,s,t}} \geq\ & 2\mathbb{R}\{\boldsymbol{\alpha}\odot \boldsymbol{Z_{i,j}}^* * \boldsymbol{S_{ij,\xi,s,t}}\} \\ & -M(1-w_{ij} * u^{\xi,t}_{ij})\ \forall i, j, ij, \xi, s, t\end{aligned} \tag{5}$$

$$\begin{aligned}\boldsymbol{W_{i,\xi,s,t}} - \boldsymbol{W_{j,\xi,s,t}} \leq\ & 2\mathbb{R}\{\boldsymbol{\alpha}\odot \boldsymbol{Z_{i,j}}^* * \boldsymbol{S_{i,j,\xi,s,t}}\} \\ & +M(1-w_{ij} * u^{\xi,t}_{ij})\ \forall i, j, ij, \xi, s, t\end{aligned} \tag{6}$$

$$(v_{lb})^2 \leq W_{i,\xi,s,t} \leq (v_{ub})^2 \quad \forall i, s, t \tag{7}$$

$$\begin{aligned}-M * w_{ij} * u^{\xi,t}_{ij} \leq P_{ij,\xi,s,t} \leq M * w_{ij} * u^{\xi,t}_{ij} \\ \forall ij, \xi, s, t\end{aligned} \tag{8}$$

$$\begin{aligned}-M * w_{ij} * u^{\xi,t}_{ij} \leq Q_{ij,\xi,s,t} \leq M * w_{ij} * u^{\xi,t}_{ij} \\ \forall i, j, ij, \xi, s, t\end{aligned} \tag{9}$$

$$\begin{aligned}\left(P^{\phi}_{ij,\xi,s,t}\right)^2 + \left(Q^{\phi}_{ij,\xi,s,t}\right)^2 \leq \left(S^{\max,\phi}_{ij,\xi,s,t}\right)^2 \\ \forall\phi\in\Phi_i, \forall ij, \xi, s, t\end{aligned} \tag{10}$$

$$\begin{aligned}P^{\phi}_{c_{i,\xi,s,t}} \leq \frac{1}{4} * \beta_i * E^{max,\phi}_b \\ \forall\phi\in\Phi_i, \forall i, \xi, s, t\end{aligned} \tag{11}$$

$$\begin{aligned}P^{\phi}_{d_{i,\xi,s,t}} \leq \frac{1}{4} * \beta_i * E^{max,\phi}_b \\ \forall\phi\in\Phi_i, \forall i, \xi, s, t\end{aligned} \tag{12}$$

$$\begin{aligned}E_{lb} * \beta_i * E^{max,\phi}_b \leq E^{\phi}_{b_{i,\xi,s,t}} \leq E_{ub} * \beta_i * E^{max,\phi}_b \\ \forall\phi\in\Phi_i, \forall i, \xi, s, t\end{aligned} \tag{13}$$

$$\begin{aligned}P^{\phi}_{b_{i,\xi,s,t}} = P^{\phi}_{c_{i,\xi,s,t}} - P^{\phi}_{d_{i,\xi,s,t}} \\ \forall\phi\in\Phi_i, \forall i, \xi, s, t\end{aligned} \tag{14}$$

$$-\frac{1}{4} * \beta_i * E_b^{max,\phi} \leq Q^{\phi}_{b_{i,\xi,s,t}} \leq \frac{1}{4} * \beta_i * E_b^{max,\phi} \quad \forall \phi \in \Phi_i, \forall i, \xi, s, t \tag{15}$$

$$E^{\phi}_{b_{i,\xi,s,t+1}} = E^{\phi}_{b_{i,\xi,s,t}} + \Delta t * \eta * P^{\phi}_{b_{i,\xi,s,t}} \quad \forall \phi \in \Phi_i, \forall i, \xi, s, t \tag{16}$$

$$E^{\phi}_{b_{i,\xi,s,0}} = E_0 \quad \forall \phi \in \Phi_i, \forall i, \xi, s, t \tag{17}$$

$$\left(P^{\phi}_{b_{i,\xi,s,t}}\right)^2 + \left(Q^{\phi}_{b_{i,\xi,s,t}}\right)^2 \leq \left(S^{\max,\phi}_{b_{i,\xi,s,t}}\right)^2 \quad \forall \phi \in \Phi_i, \forall i, \xi, s, t \tag{18}$$

$$0 \leq P^{shed,\phi}_{i,\xi,s,t} \leq P^{\phi}_{L_{i,\xi,s,t}} \quad \forall \phi \in \Phi_i, \forall i, \xi, s, t \tag{19}$$

$$w_{i,j} = 1 \quad \forall ij \in L^E \tag{20}$$

$$w_{i,j} \in \{0, 1\} \quad \forall ij \tag{21}$$

$$\beta_i \in \mathbb{N}^0 \quad \forall i \tag{22}$$

where,

$$\boldsymbol{\alpha} = \begin{bmatrix} 1 & e^{j*pi/3} & e^{-j*\pi/3} \\ e^{-j*\pi/3} & 1 & e^{j*\pi/3} \\ e^{-j*\pi/3} & e^{j*\pi/3} & 1 \end{bmatrix} \tag{23}$$

The objective function (1) minimizes the sum of the investment cost in the first stage, which includes the cost of new lines and ESSs, and the operation cost in the second stage, which includes the operation and maintenance cost of ESSs, the cost of energy, and the cost of load shedding at each node.

This model adopted an unbalanced three-phase linear branch flow method, assuming that branch power losses are relatively smaller as compared to the branch power flow and that the obtained feeder voltages are a good approximation of the actual feeder voltages [37]. Constraints (3) and (4) enforce the power balance at each node only if the line is available (i.e., $u_{i,j} = 1$). The line availability is established depending on whether the branch is in an HFTD Zone or not. Constraints (5) and (6) calculate the voltage at every node i. The Big-M formulation is used to guarantee that the constraints are active only when the corresponding binary variables are equal to 1. The procedure to determine the proper M value can be found in [38]. Constraint (7) enforces the upper and lower bonds of the voltage in each node.

Constraints (8) and (9) enforce that there is only active and reactive power, respectively, flowing on the potential new lines that are built. The capacity of the transformers is determined by their rated kVA capacity, and the capacity of the lines by their ampacity at rated voltage. Constraint (10) guarantees that the loading on the transformers and lines are restrained to its $\mathbf{S^{max}}$.

Constraints (11) to (17) are related to the operation of the ESSs. The presented ESS operation model is obtained from the work in [39], where new linear constraints are proposed to optimally dispatch batteries while guaranteeing the satisfaction of SoC constraints without having to resort to binary variables for the charging/discharging dynamics, thus greatly reducing the complexity of the ESSs formulation. Constraints (11), (12), and (15) limit the ESSs active power charging, discharging, and reactive power to 1/4 of its total capacity per hour, respectively. Constraint (13) enforces that the ESSs energy operates within its lower and upper bounds. Constraint (16) presents the energy calculation of all time steps. Constraint (17) enforces that all ESSs have the same initial value stored. Constraint (18) guarantees that the loading on the ESSs restrained to its $S^{max}_{b_i}$.

The fact that the existing lines have already been built is enforced by Constraint (20). Constraint (19) establishes that it is not possible to shed more load than is demanded at each node. Constraints (21) defines the variables $w_{i,j}$ as binary. Constraint (22) defines the variables β_i as integers greater or equal to zero. Finally, Constraint (23) defines the $\boldsymbol{\alpha}$ matrix, a necessary operator to represent the diagonal and off-diagonal contribution of $\boldsymbol{Z_{i,j}}$, which is used to properly calculate the voltage drop across a line for the unbalanced three-phase linear branch flow method [37].

Note that (10) is quadratic. Thus, a polygon-based linearization method [40] is used to approximate the quadratic terms. The radius of the polygon is presented in (24), and the linear constraints when n = 6 can be formulated as presented in (25)-(27). Constraint (18), which is also quadratic, is linearized in the same manner.

$$S^{\phi,H}_{ij} = S^{\max}_{ij} \sqrt{\frac{2\pi}{n} \sin(\frac{2\pi}{n})} \quad \forall \phi \in \Phi_i, \forall ij \tag{24}$$

$$Q^{\phi}_{ij,\xi,s,t} \geq -\sqrt{3}\left(P^{\phi}_{ij,\xi,s,t} + S^{\phi,H}_{ij}\right)$$
$$Q^{\phi}_{ij,\xi,s,t} \leq -\sqrt{3}\left(P^{\phi}_{ij,\xi,s,t} - S^{\phi,H}_{ij}\right) \quad \forall \phi \in \Phi_i, \forall ij, \xi, s, t \tag{25}$$

$$-\frac{\sqrt{3}}{2} S^{\phi,H}_{ij} \leq Q^{\phi}_{ij,\xi,s,t} \leq \frac{\sqrt{3}}{2} S^{\phi,H}_{ij} \quad \forall \phi \in \Phi_i, \forall ij, \xi, s, t \tag{26}$$

$$Q^{\phi}_{ij,\xi,s,t} \geq \sqrt{3}\left(P^{\phi}_{ij,\xi,s,t} - S^{\phi,H}_{ij}\right)$$
$$Q^{\phi}_{ij,\xi,s,t} \leq \sqrt{3}\left(P^{\phi}_{ij,\xi,s,t} + S^{\phi,H}_{ij}\right) \quad \forall \phi \in \Phi_i, \forall ij, \xi, s, t \tag{27}$$

III. CASE STUDIES

The proposed model has been applied to a modified IEEE 13-node and IEEE-123-node system [41], on an AMD Ryzen 5 3500U with Radeon Vega Mobile Gfx 2.10 GHz-based processor with 8 GB of RAM using Julia along with the Julia for Mathematical Programming (JuMP) package [42], and Gurobi 7.0 [43]. The data for every distribution system corridor was obtained from [41].

A. DATA AND ASSUMPTIONS

The cost of constructing overhead and underground lines was obtained from [44], being on average $433.07, and $2,952.76 per meter, respectively. Three scenarios with equal

TABLE 2. Number of events and average outage time of the PSPS events, obtained from PG&E [48].

Year	2019	2020	2021
Number of events	7	5	4
Average outage time (h)	57	40.1	29.6

probability were used to model the average outage time and number of PSPS events, based on real-world data from PG&E that reflect three distinct wildfire seasons (i.e., 2019, 2020, and 2021). The number of PSPS events per year and the average outage time of the PSPS events considered are presented in Table 2. Moreover, three representative days are chosen to build the load profiles for a typical winter, summer, and spring day. In order to get a better representation during the wildfire season, an entire week is chosen for this period.

The cost of generation and load shedding is solved for those windows of time, hourly based. Thus, the cost of shedding the load and generation is multiplied by the number of years N, and the weighting factor, σ_s. The planning horizon, N, is considered to be 10 years. The hourly load data is equal to the multiplication of peak load data and hourly load factor curve that is presented in Fig. 3(a), Fig. 3(b), Fig. 3(c), and Fig. 3(d), for the spring, summer, wildfire season, and the winter, respectively, obtained from [45], considering the Portland General Electrical (PGE) balancing authority. The days selected are the 16th of January, April, and July, and the week for the wildfire season was September 16th-22nd.

The energy price considered was obtained from the California Independent System Operator (CAISO) DNCR_LNODEBR1 node [46], in 2020, and 2021, during the same days as the load curves were obtained. The energy price for 2019 was not available, thus 2021 data is used for 2019.

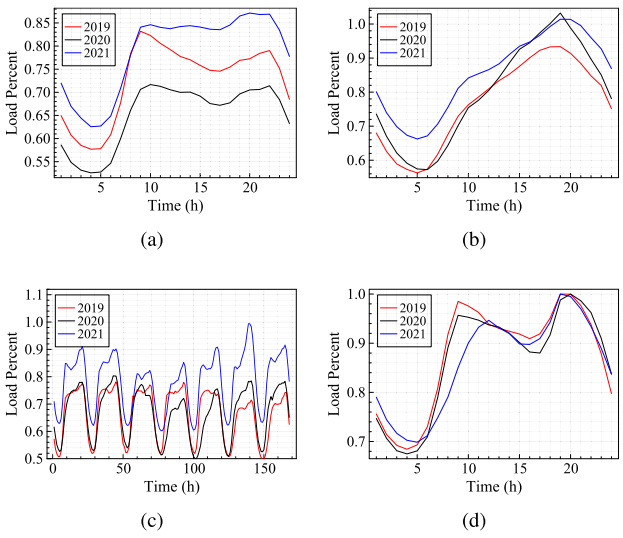

FIGURE 3. Load percent curve during the (a) spring, (b) summer, (c) wildfire season and (d) winter, for the years of 2019, 2020, and 2021.

TABLE 3. Operational information of ESS units.

Parameter	Value
Technology	Lithium-Ion
Capacity per module	60 kWh
Unit cost for power rating	200 $/kWh
Fixed O&M cost per module	20 $/day
Efficiency	95%
SOC limits	20-80%
Initial SOC status	50%

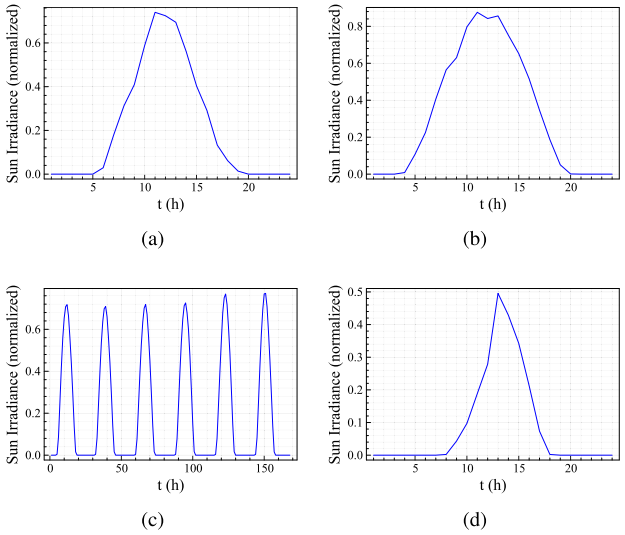

FIGURE 4. Normalized sun irradiance curve during the (a) spring, (b) summer, (c) wildfire season, and (d) winter.

To analyze the integration of HFTD Zones on the proposed power distribution system expansion formulation, the study was performed considering the following assumptions:

1) The underground lines are not affected by the wildfires.
2) The new node should be supplied by a three-phase distribution line.
3) All overhead lines that can be connected to the new nodes are within an HFTD Tier 2 or 3.

The parameters used for the ESS were obtained from [47] and are presented in Table 3.

The potential lines and ESS candidate nodes were selected if they have all three phases and based on their location, i.e., geographically close to the new node and electrically close to or at a node that contains DG, respectively. For both systems, photovoltaic (PV) DG was considered to be previously installed on the system. The PVWatts model was used to calculate the power output. The sun irradiance was obtained from [49], and it was considered the same for all the scenarios. The normalized (for a 1000W/m^2 reference) hourly data is presented in Fig. 4(a), Fig. 4(b), Fig. 4(c), and Fig. 4(d), for the spring, summer, wildfire season, and the winter, respectively.

For both distribution test systems, random moments during the wildfire season are generated to be considered PSPS events.

TABLE 4. Characteristics of potential new lines.

Line	Length (m)	Line Configuration	Construction
Line 632, 635	314.2	601	Overhead
Line 671, 635	314.2	601	Overhead
Line 633, 635	314.2	602	Overhead
Line 634, 635	314.2	602	Overhead
Line 692, 635	314.2	606	Underground
Line 675, 635	314.2	606	Underground

B. RESULTS: IEEE 13-NODE SYSTEM

The IEEE-13 node system with the newly created node and its potential connections is presented in Fig. 5. Node 635 is created with an unbalanced load obtained from the average of all the other nodes in the system. The characteristics and parameters of the potential new lines are presented in Table 4. Table 5 presents both the DG and ESS nodes information for the IEEE 13-node system. The DG modules have a 60kWh capacity per phase.

By considering that no outages happened in any of the scenarios, the obtained optimal solution cost is $ 10,059,052.09, and the line selected to be built is the connection between node 671 and the new node, 635, given the lower cost of the overhead lines in comparison with underground lines [44]. However, when considering that overhead lines that are within HFTD Tier zones 2 or 3 are likely to be unavailable during certain periods of the wildfire season, the optimal solution is highly impacted by how much it costs to shed the load at node 635 *vs* the cost of undergrounding the connection.

Without considering the possibility of ESSs, with a $VoLL = 2\$/kWh$, and considering the overhead lines within HFTD Tier zones 2 or 3 unavailability during certain periods of the wildfire season, the optimal solution cost is $10,850,688.37, selecting the underground option to connect the node 692 to the new node 635. However, considering the ESS candidate nodes presented in Fig. 5, the optimal solution cost is reduced to $10,627,195.27, selecting the previous branch (node 671 to node 635), and installing three 3ϕ ESSs modules at node 635. During moments of unavailability of the line between nodes 671 and 635, the load is supplied by the three ESS modules installed at node 635. Fig. 6 presents the load shed, the ESS SOC, and the battery charging/discharging dynamics during moments of unavailability, for phase A.

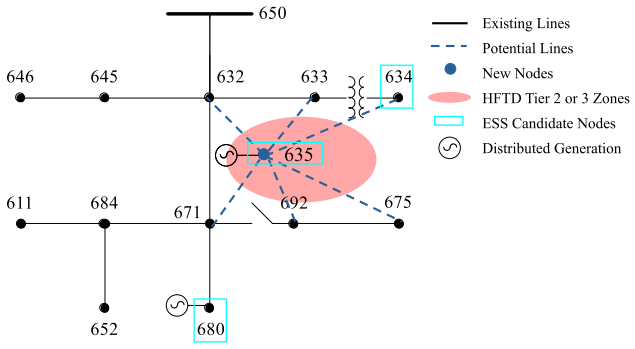

FIGURE 5. Modified IEEE 13-node system including the new node and the potential new lines.

TABLE 5. DG nodes and ESS candidate nodes for the IEEE 13-node system.

DG nodes	4, 14
ESS candidate nodes	4, 8, 14

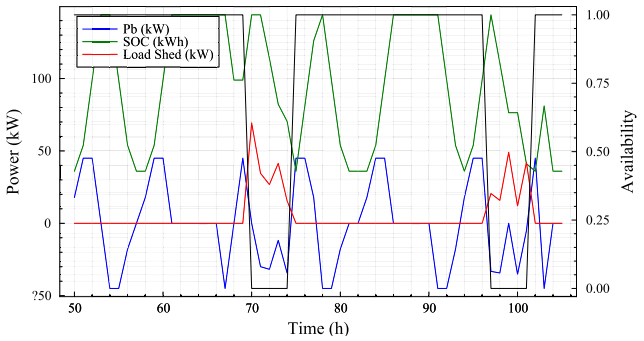

FIGURE 6. Time *vs* battery charging/discharging dynamics, SoC, and load shedding at node 635 during the two first wildfire risk events, for the first scenario (year 2019).

TABLE 6. Final solutions from the sensitivity analysis of the distribution expansion problem for IEEE 13-node system.

VoLL ($/kWh)	2	4	6	8
Number of new overhead lines	2	2	2	1
Number of new underground lines	0	0	0	1
Total ESS capacity (kWh/phase)	180	420	480	0
Total P^{shed}/year (kWh)	15,484.12	2,800.97	1,126.78	3,172.94
Solution Cost (10^6 $)	10.63	10.79	10.84	10.85

Regardless of the presence of the ESS, there might be a need for load shedding during wildfire risk events, depending on the value of the *VoLL*. Thus, a sensitivity analysis is performed to analyze the impact of the parameter on the final solution.

Fig. 7 presents the effect of the *VoLL* parameter on the solution's final value. Fig. 8 presents the effect on the average load shedding per year at node 14. The *VoLL* values used are $VoLL = \{2, 4, 6, 8\}\$/kWh$. The optimal cost is normalized and related to the solution considering that no outages happened in any of the scenarios. The final solutions for the sensitivity analysis are presented in Table 6.

For a $VoLL = \{2, 4, 6\}\$/kWh$, the overhead line connecting the node 671 to 635 is chosen, however, when the cost of shedding the load is equal to $8.00 per kWh, the solution changes to an underground option, connecting the node 692 to the node 635. Thus, the price to shed the load has an extreme impact on the final decision.

Although for smaller values of *VoLL*, the optimal solution is to jointly construct an overhead line, which will be exposed to unavailability during certain moments of the year, and install ESSs, the difference is less than 3% when comparing

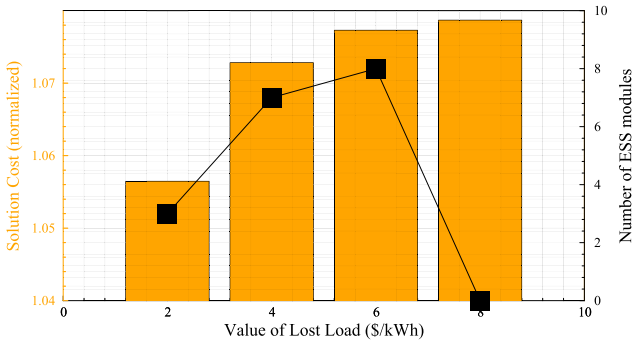

FIGURE 7. Sensitivity analysis on the impact of the *VoLL* parameter on the solution cost for the IEEE 13-node system.

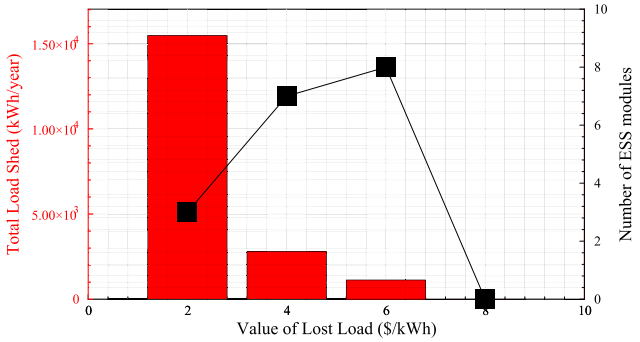

FIGURE 8. Sensitivity analysis on the impact of the *VoLL* parameter on the load shedding per year for the IEEE 13-node system.

TABLE 7. Characteristics of new potential lines.

Line	Length (m)	Line Configuration	Construction
Line 51, 125	91.44	4	Overhead
Line 65, 125	129.54	12	Underground
Line 151, 125	152.4	4	Overhead
Line 56, 126	182.88	1	Overhead
Line 76, 126	213.36	11	Overhead
Line 610, 126	106.68	12	Underground

to an underground solution, which would be expected to be available during moments of wildfire risk.

C. RESULTS: IEEE 123-NODE SYSTEM

The proposed model was also validated using the IEEE-123 node system. Fig. 9 shows the system to be expanded considering the newly created nodes and their potential connections. The new nodes 125 and 126 are created with an unbalanced load obtained from the average of all the other nodes in the system. The characteristics and parameters of the potential new lines are presented in Table 7. Table 8 presents both the DG and ESS information for the modified IEEE 123-node system. The DG modules have a 60kWh capacity per phase.

By considering that no outages happened in any of the scenarios, the obtained optimal solution cost is \$9,754,971.61, selecting the lowest-cost overhead options, connecting node 51 to the new node 125 and node 56 to the new node 126.

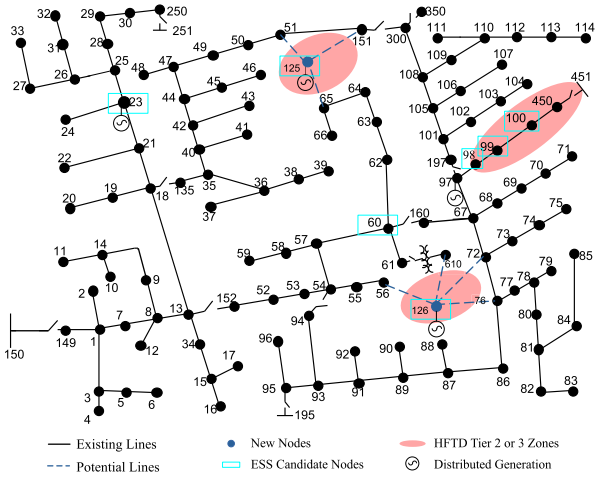

FIGURE 9. IEEE 123-node system including the new nodes 125 and 126.

TABLE 8. DG nodes and ESS candidate nodes for the IEEE 123-node system.

DG nodes	23, 97, 125, 126
ESS candidate nodes	23, 60, 98, 99, 100, 125, 126

Without considering the possibility of ESSs, with a $VoLL = 2\$/kWh$, and considering the overhead lines within HFTD Tier zones 2 or 3 unavailability during certain periods of the wildfire season, the optimal solution cost is \$10,578,069.23. This solution considers underground lines to connect the nodes 65 and 125 as well as the nodes 610 and 126. However, considering the ESS candidate nodes presented in Fig. 9, the optimal solution cost is reduced to \$10,517,574.17, selecting a combination of three ESS modules and an overhead option for node 125 (node 51 to 125), and the underground option for the node 126. That is, the difference is less than \$61,000 (less than 0.1% when compared to the reference) when comparing to an underground solution, that is to be available during all moments of wildfire risk, but the demand at nodes 99 and 100 is still completely shed.

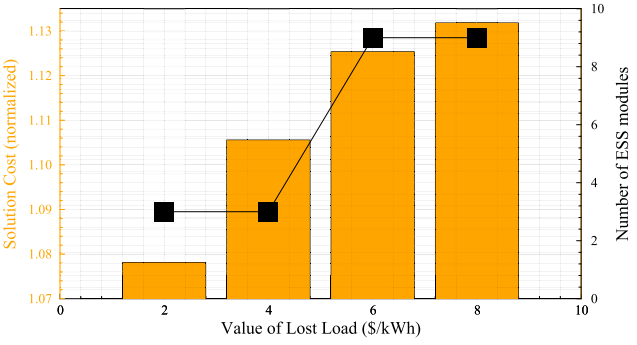

FIGURE 10. Sensitivity analysis on the impact of the *VoLL* parameter on the solution cost for the IEEE 123-node system.

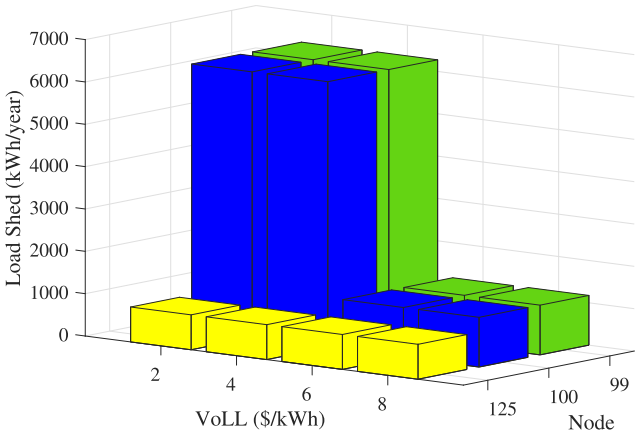

FIGURE 11. Sensitivity analysis on the impact of the *VoLL* parameter on the load shedding per year for IEEE 123-node system.

TABLE 9. Final solutions from the sensitivity analysis of the distribution expansion problem for IEEE 123-node system.

VoLL ($/kWh)	2	4	6	8
Number of new overhead lines	1	1	1	1
Number of new underground lines	1	1	1	1
Total ESS capacity (kWh/phase)	180	180	540	540
Total P^{shed}/year (kWh)	13,373.69	13,373.69	3172.94	3172.94
Solution Cost (10^6 $)	10.52	10.79	10.98	11.04

The same sensitivity analysis for the *VoLL* is performed for the modified version of the IEEE 123-node system. Fig. 10 presents the effect of the *VoLL* parameter on the total system cost. Fig. 11 presents the effect of the *VoLL* on the total load shedding per year. The *VoLL* values used are $VoLL = \{2, 4, 6, 8\}\$/kWh$. The optimal cost is normalized and related to the solution considering that no outages happened in any of the scenarios. The final solutions for the sensitivity analysis are presented in Table 9.

For the cases where $VoLL = \{2, 4\}\$/kWh$, three ESSs are installed only at node 125, and during wildfire risk moments all the demand at nodes 99 and 100 is shed. Increasing the *VoLL* to \$6/kWh and \$8/kWh, other three ESS modules are installed at the nodes 99 and 100 totaling nine ESS modules, reducing significantly the average of load shedding per year. However, the decision on which distribution lines to be constructed does not change with this parameter. Thus, for the modified version of the IEEE 123-node system, the integration of ESS provides an intriguing solution, proving to be more valuable for one of the nodes even when the cost of load shed gets 4 times the baseline value.

To analyze the impact of considering ESS on the distribution expansion planning problem, the same sensitivity analysis is conducted comparing the final solution cost and total load shed with and without ESSs for the IEEE 123-node system. Without considering ESSs, the expansion decisions are to construct underground distribution lines for both new nodes, 125 and 116 for all *VoLL* values considered, that is, constructing the distribution lines from node 65 to node 125 and from node 610 to node 126.

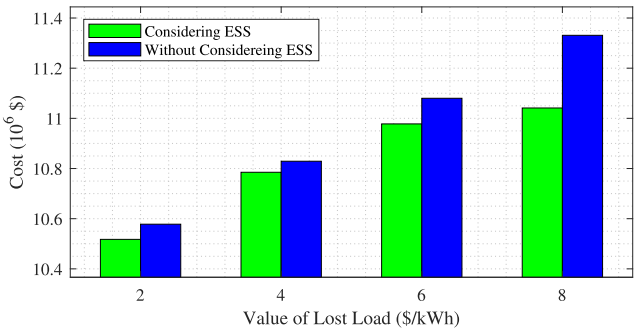

FIGURE 12. Sensitivity analysis on the impact of the *VoLL* parameter and the presence of ESS on the solution cost for IEEE 123-node system.

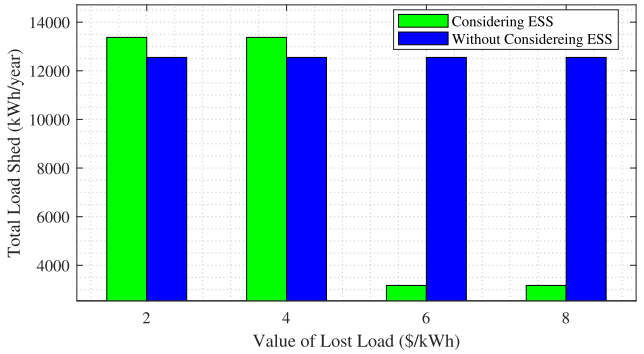

FIGURE 13. Sensitivity analysis on the impact of the *VoLL* parameter and the presence of ESS on the load shedding per year for IEEE 123-node system.

Fig. 12 and Fig. 13 present effect of the *VoLL* parameter on the total system cost and on the total load shedding per year, respectively. The solution without evaluating ESSs was more expensive for all values of *VoLL* considered, getting significantly greater for larger values of *VoLL*, due to the fact that the load at the nodes 98, 99, and 100 cannot be supplied during the wildfire season. For the cases where $VoLL = \{2, 4\}\$/kWh$, the total load shed per year is around 820 kWh less without considering ESSs when compared the solution that jointly install 3 modules on node 125 and an overhead line from node 51 to 125. Nevertheless, for larger values of *VoLL* the investment of 3 modules at node 99 and 3 modules at node 100 majorly reduces the total load shed by almost 75%, making the alternative of ESSs on the distribution system expansion planning very appealing.

IV. CONCLUSION

This work proposed a two-stage stochastic optimization framework for the unbalanced distribution system expansion and energy storage planning that takes into account the wildfire risk. The wildfire risk representation was modeled as the unavailability of the specific lines that are within HFDT Tier Zones. The problem was solved for the IEEE 13-node system and the IEEE 123-node system, using the unbalanced linearized load flow, including a linear formulation of the optimal battery charging-discharging dynamics, with

a seasonal load variation and hourly price, for a horizon of 10 years. For the IEEE 13-node system, the solution varied as the *VoLL* parameter is changed, indicating the point where is cost-beneficial to construct the underground solution. Although the solution varied for the IEEE 123-node system, only moments where more ESSs are decided to be constructed were identified, proving that jointly expanding the system with the inclusion of ESSs can be more beneficial than undergrounding.

Future studies can be conducted to incorporate other alternatives to investigate the mitigation of the wildfire risk, such as line hardening, vegetation management, and microgrid formation during wildfire risk moments. Moreover, a robust optimization scheme can be developed considering a robust set of the average, and standard deviation of the outage time within HFTD Tier zones, without relying on historical data for de-energization scenarios.

REFERENCES

[1] A. Witze, "The Arctic is burning like never before—And that's bad news for climate change," *Nature*, vol. 585, no. 7825, pp. 336–337, Sep. 2020.

[2] K. Wheeling, "Australia's most extreme bushfire season, statistically speaking," *Eos*, vol. 101, Nov. 2020. Accessed: Apr. 5, 2023, doi: 10.1029/2020EO151949.

[3] E. Logiuratto. (2020). *Desperate Race Against Fires in World's Biggest Tropical Wetlands*. Accessed: Dec. 21, 2021. [Online]. Available: https://phys.org/news/2021-01-brazil-wildfires-surge.html

[4] NIFC. (2020). *National Fire News*. Accessed: Dec. 21, 2021. [Online]. Available: https://www.nifc.gov/fire-information/nfn

[5] M. J. Case, B. G. Johnson, K. J. Bartowitz, and T. W. Hudiburg, "Forests of the future: Climate change impacts and implications for carbon storage in the Pacific Northwest, USA," *Forest Ecology Manag.*, vol. 482, Feb. 2021, Art. no. 118886.

[6] J. T. Abatzoglou and C. A. Kolden, "Climate change in western US deserts: Potential for increased wildfire and invasive annual grasses," *Rangeland Ecology Manag.*, vol. 64, no. 5, pp. 471–478, Sep. 2011.

[7] Y. Liu, S. L. Goodrick, and J. A. Stanturf, "Future US wildfire potential trends projected using a dynamically downscaled climate change scenario," *Forest Ecology Manag.*, vol. 294, pp. 120–135, Apr. 2013. [Online]. Available: https://www.sciencedirect.com/science/article/pii/S037811271200388X

[8] P. Brando, M. Macedo, D. Silvério, L. Rattis, L. Paolucci, A. Alencar, M. Coe, and C. Amorim, "Amazon wildfires: Scenes from a foreseeable disaster," *Flora*, vol. 268, Jul. 2020, Art. no. 151609. [Online]. Available: https://www.sciencedirect.com/science/article/pii/S0367253020300736

[9] M. E. Rocca, C. F. Miniat, and R. J. Mitchell, "Introduction to the regional assessments: Climate change, wildfire, and forest ecosystem services in the USA," *Forest Ecol. Manag.*, vol. 327, pp. 265–268, Mar. 2014.

[10] J. K. Summers, A. Lamper, C. Mcmillion, and L. C. Harwell, "Observed changes in the frequency, intensity, and spatial patterns of nine natural hazards in the United States from 2000 to 2019," *Sustainability*, vol. 14, no. 7, p. 4158, Mar. 2022. [Online]. Available: https://www.mdpi.com/2071-1050/14/7/4158

[11] S. Gonick and N. Errett, "Integrating climate change into hazard mitigation planning: A survey of state hazard mitigation officers," *Sustainability*, vol. 10, no. 11, p. 4150, Nov. 2018. [Online]. Available: https://www.mdpi.com/2071-1050/10/11/4150

[12] NCEI. (2023). *NOAA National Centers for Environmental Information US Billion-Dollar Weather and Climate Disasters (2023)*. [Online]. Available: https://www.ncei.noaa.gov/access/billions/

[13] A. Ganteaume, R. Barbero, M. Jappiot, and E. Maillé, "Understanding future changes to fires in southern Europe and their impacts on the wildland-urban interface," *J. Saf. Sci. Resilience*, vol. 2, no. 1, pp. 20–29, Mar. 2021. [Online]. Available: https://www.sciencedirect.com/science/article/pii/S2666449621000013

[14] S. A. Parks, L. M. Holsinger, K. Blankenship, G. K. Dillon, S. A. Goeking, and R. Swaty, "Contemporary wildfires are more severe compared to the historical reference period in western US dry conifer forests," *Forest Ecology Manag.*, vol. 544, Sep. 2023, Art. no. 121232. [Online]. Available: https://www.sciencedirect.com/science/article/pii/S0378112723004668

[15] EPRI. (2021). *EPRI Wildfire Mitigation Planning: Research and Applications*. [Online]. Available: https://www.epri.com/research/products/000000003002022665

[16] PG&E. (2020). *Pacific Gas and Electric Company (PG&E) Wildfire Safety*. Accessed: Dec. 21, 2021. [Online]. Available: https://www.pge.com/en_US/safety/emergencypreparedness/natural-disaster/wildfires/wildfire-safety.page?WT.mc_id=Vanity_wildfiresafety

[17] PacifiCorp. *PacifiCorp 2021 PSPS Performance*. Accessed: Jun. 5, 2023. [Online]. Available: https://www.cpuc.ca.gov/-/media/cpuc-website/divisions/safety-and-enforcement-division/meeting-documents/psps-briefings-february-2022/pacificorp-ca-psps-briefing-presentation-feb-2022.pdf

[18] CPU Commission. *Fire-Threat Maps and Fire-Safety Rulemaking*. Accessed: Jul. 6, 2023. [Online]. Available: https://www.cpuc.ca.gov/industries-and-topics/wildfires/fire-threat-maps-and-fire-safety-rulemaking

[19] P. Murphy. (2021). *Preventing Wildfires With Power Outages: The Growing Impacts of California's Public Safety Power Shutoffs*. [Online]. Available: https://www.psehealthyenergy.org/news/blog/preventing-wildfires-with-power-outages-2/

[20] PG&E. (2022). *Wildfire Mitigation Plan*. Accessed: Mar. 21, 2023. [Online]. Available: https://www.pge.com/en_US/safety/emergency-preparedness/natural-disaster/wildfires/wildfire-mitigation-plan.page?WT.mc_id=Vanity_wildfiremitigationplan

[21] J. Keen, J. Giraldez, E. Cook, A. Eiden, S. Placide, A. Hirayama, B. Monson, D. Mino, and F. Eldali, "Distribution capacity expansion planning: Current practice, opportunities, and decision support," Nat. Renew. Energy Lab. (NREL), Golden, CO, USA, Tech. Rep. NREL/TP-6A40-83892, 2022.

[22] G. L. Aschidamini, G. A. da Cruz, M. Resener, M. J. S. Ramos, L. A. Pereira, B. P. Ferraz, S. Haffner, and P. M. Pardalos, "Expansion planning of power distribution systems considering reliability: A comprehensive review," *Energies*, vol. 15, no. 6, p. 2275, Mar. 2022.

[23] S. S. Tanwar and D. K. Khatod, "A review on distribution network expansion planning," in *Proc. Annu. IEEE India Conf. (INDICON)*, Dec. 2015, pp. 1–6.

[24] S. Mohagheghi and S. Rebennack, "Optimal resilient power grid operation during the course of a progressing wildfire," *Int. J. Electr. Power Energy Syst.*, vol. 73, pp. 843–852, Dec. 2015. [Online]. Available: https://www.sciencedirect.com/science/article/pii/S0142061515002409

[25] D. N. Trakas and N. D. Hatziargyriou, "Optimal distribution system operation for enhancing resilience against wildfires," *IEEE Trans. Power Syst.*, vol. 33, no. 2, pp. 2260–2271, Mar. 2018.

[26] M. Nazemi, P. Dehghanian, M. Alhazmi, and Y. Darestani, "Resilience enhancement of electric power distribution grids against wildfires," in *Proc. IEEE Ind. Appl. Soc. Annu. Meeting (IAS)*, Oct. 2021, pp. 1–7.

[27] M. Nazemi and P. Dehghanian, "Powering through wildfires: An integrated solution for enhanced safety and resilience in power grids," *IEEE Trans. Ind. Appl.*, vol. 58, no. 3, pp. 4192–4202, May 2022.

[28] M. Nazemi, P. Dehghanian, M. Alhazmi, and Y. Darestani, "Resilient operation of electric power distribution grids under progressive wildfires," *IEEE Trans. Ind. Appl.*, vol. 58, no. 2, pp. 1632–1643, Mar. 2022.

[29] S. Tandon, S. Grijalva, and D. K. Molzahn, "Motivating the use of dynamic line ratings to mitigate the risk of wildfire ignition," in *Proc. IEEE Power Energy Conf. at Illinois (PECI)*, Apr. 2021, pp. 1–7.

[30] T. Tapia, Á. Lorca, D. Olivares, M. Negrete-Pincetic, and A. J. Lamadrid L, "A robust decision-support method based on optimization and simulation for wildfire resilience in highly renewable power systems," *Eur. J. Oper. Res.*, vol. 294, no. 2, pp. 723–733, Oct. 2021. [Online]. Available: https://www.sciencedirect.com/science/article/pii/S0377221721000862

[31] A. Lesage-Landry, F. Pellerin, J. A. Taylor, and D. S. Callaway, "Optimally scheduling public safety power shutoffs," 2022, *arXiv:2203.02861*.

[32] N. Rhodes, L. Ntaimo, and L. Roald, "Balancing wildfire risk and power outages through optimized power shut-offs," *IEEE Trans. Power Syst.*, vol. 36, no. 4, pp. 3118–3128, Jul. 2021.

[33] A. Kody, A. West, and D. K. Molzahn, "Sharing the load: Considering fairness in de-energization scheduling to mitigate wildfire ignition risk using rolling optimization," in *Proc. IEEE 61st Conf. Decis. Control (CDC)*, Dec. 2022, pp. 5705–5712.

[34] A. Kody, R. Piansky, and D. K. Molzahn, "Optimizing transmission infrastructure investments to support line de-energization for mitigating wildfire ignition risk," 2022, *arXiv:2203.10176*.
[35] A. Zanin Bertoletti and J. Campos do Prado, "Transmission system expansion planning under wildfire risk," in *Proc. North Amer. Power Symp. (NAPS)*, Oct. 2022, pp. 1–6.
[36] R. Bayani and S. D. Manshadi, "Resilient expansion planning of electricity grid under prolonged wildfire risk," *IEEE Trans. Smart Grid*, vol. 14, no. 5, pp. 3719–3731, Sep. 2023.
[37] L. Gan and S. H. Low, "Convex relaxations and linear approximation for optimal power flow in multiphase radial networks," in *Proc. Power Syst. Comput. Conf.*, Aug. 2014, pp. 1–9.
[38] M. S. Bazaraa, J. J. Jarvis, and H. D. Sherali, *Linear Programming and Network Flows*. Hoboken, NJ, USA: Wiley, 2011.
[39] N. Nazir and M. Almassalkhi, "Guaranteeing a physically realizable battery dispatch without charge-discharge complementarity constraints," *IEEE Trans. Smart Grid*, vol. 14, no. 3, pp. 2473–2476, May 2023.
[40] H. Ahmadi and J. R. Marti, "Linear current flow equations with application to distribution systems reconfiguration," *IEEE Trans. Power Syst.*, vol. 30, no. 4, pp. 2073–2080, Jul. 2015.
[41] K. P. Schneider, B. A. Mather, B. C. Pal, C.-W. Ten, G. J. Shirek, H. Zhu, J. C. Fuller, J. L. R. Pereira, L. F. Ochoa, L. R. de Araujo, R. C. Dugan, S. Matthias, S. Paudyal, T. E. McDermott, and W. Kersting, "Analytic considerations and design basis for the IEEE distribution test feeders," *IEEE Trans. Power Syst.*, vol. 33, no. 3, pp. 3181–3188, May 2018.
[42] I. Dunning, J. Huchette, and M. Lubin, "JuMP: A modeling language for mathematical optimization," *SIAM Rev.*, vol. 59, no. 2, pp. 295–320, Jan. 2017.
[43] Gurobi Optimization. LLC. (2022). *Gurobi Optimizer Reference Manual*. [Online]. Available: https://www.gurobi.com
[44] CPUC. (2022). *Undergrounding Programs Description*. [Online]. Available: https://www.cpuc.ca.gov/industries-and-topics/electrical-energy/infrastructure/electric-reliability/undergrounding-program-description
[45] EIA. (2022). *Hourly Electric Grid Monitor*. [Online]. Available: https://www.eia.gov/electricity/gridmonitor/dashboard/electric_overview/
[46] CAISO. (2022). *California ISO—Locational Marginal Price*. [Online]. Available: http://oasis.caiso.com/mrioasis/logon.do#
[47] J. H. Yi, R. Cherkaoui, M. Paolone, D. Shchetinin, and K. Knezovic, "Expansion planning of active distribution networks achieving their dispatchability via energy storage systems," *Appl. Energy*, vol. 326, Nov. 2022, Art. no. 119942. [Online]. Available: https://www.sciencedirect.com/science/article/pii/S0306261922011990
[48] PG&E. (2022). *PSPS Reports*. [Online]. Available: https://www.pge.com/en_US/residential/outages/public-safety-power-shuttoff/psps-reports.page
[49] WSU. (2021). *Agweathernet*. Accessed: Dec. 22, 2021. [Online]. Available: http://weather.wsu.edu/?p=88650&desktop

AUGUSTO ZANIN BERTOLETTI (Member, IEEE) was born in Passo Fundo, Brazil, in 1998. He received the B.Eng. degree in electrical engineering from the Federal University of Santa Maria, Santa Maria, Brazil, in 2020, and the M.S. degree in electrical engineering from Washington State University at Vancouver, Vancouver, WA, USA, in 2023. His current research interests include distributed energy resources, power systems planning and operation, power systems analysis and protection, and optimization under uncertainty applied to power systems. He has received the 2023 IEEE Power and Energy Society (PES) Outstanding Student Scholarship for his academic achievements, contributions to meeting community and humanitarian needs, and leadership in advancing student engagement within PES.

JOSUE CAMPOS DO PRADO (Member, IEEE) was born in Joinville, Brazil, in 1989. He received the B.Eng. degree in electrical engineering from Santa Catarina State University, Joinville, in 2012, and the Ph.D. degree in electrical engineering from the University of Nebraska–Lincoln, Lincoln, NE, USA, in 2020. He conducted research on power system resilience and flexibility with the National Renewable Energy Laboratory (NREL), Joint Institute for Strategic Energy Analysis (JISEA), from October 2018 to July 2020. Since August 2020, he has been with Washington State University at Vancouver, Vancouver, WA, USA, where he is currently an Assistant Professor with the School of Engineering and Computer Science. His current research interests include distributed energy resources, power systems planning and operation, and optimization under uncertainty applied to power systems.